Ion-Controlled Collisionless Magnetic Reconnection

D. Biskamp and E. Schwarz
Max-Planck-Institut für Plasmaphysik, 85748 Garching, Germany

J. F. Drake
Institute for Plasma Research, University of Maryland, College Park, Maryland 20742
(Received 22 June 1995)

A theory of fast collisionless reconnection is presented. Because of the Hall term in Ohm's law, electron and ion dynamics decouple on scales smaller than the ion inertial length c/ω_{pi}. Though reconnection requires electron inertia to break the frozen-flux constraint, the rate is essentially independent of the electron mass. Instead, ion inertia controls the reconnection rate, which is strongly enhanced compared to previous estimates in which Hall effects were neglected.

PACS numbers: 52.30.–q, 52.65.Kj

Observations in space and laboratory devices indicate that fast magnetic reconnection processes may occur in nearly collisionless plasmas. For instance, the time scales of the sawtooth collapse in tokamaks are much faster than can be accounted for by weak collisional effects such as resistivity and electron viscosity [1]. Even more stunning are the rapid processes observed in the magnetosphere, where plasmas are virtually collisionless. In a collisionless plasma electron inertia enables the frozen-flux constraint to be broken and reconnection to proceed [2–4]. Reconnection takes place in a narrow region around an X point of the magnetic configuration [5], the diffusion region. In the collisionless limit, the characteristic scale length of this region is of order $d_e = c/\omega_{pe}$. It has recently been shown that at scale lengths smaller than $d_i = c/\omega_{pi} \gg d_e$ the Hall term allows the electron and ion motion to decouple [6]. Thus, a proper treatment of collisionless reconnection must include both electron inertia and the Hall term and properly resolve and separate the scales d_e, d_i and the macroscale L. We show that the decoupling of the electron and ion motion in the diffusion region leads to strongly enhanced reconnection rates. In the present Letter we focus on a high-β system, where the axial magnetic field component is small. The results strongly suggest, however, that previous theories of reconnection in systems with a strong axial magnetic field must also be reevaluated [3,4].

For distances from the reconnection point smaller than d_i the ions can be considered immobile and the dynamics is due only to the electrons moving in their self-consistent electromagnetic fields, which are described by electron magnetohydrodynamics (EMHD) [7–9]. In 2D the EMHD equations can be written in terms of two scalar quantities, the flux function ψ describing the poloidal magnetic field $\mathbf{B} = \hat{\mathbf{z}} \times \nabla\psi$, and $\varphi_e = \delta B_z$, the fluctuation of the axial field, which acts as a stream function of the poloidal electron velocity $\mathbf{v}_e = \hat{\mathbf{z}} \times \nabla\varphi_e$:

$$\partial_t(\psi - d_e^2 j) + \mathbf{v}_e \cdot \nabla(\psi - d_e^2 j) = (-1)^{\nu-1}\eta_\nu \nabla^{2(\nu-1)} j\,, \tag{1}$$

$$\partial_t(\varphi_e - d_e^2\omega_e) + \mathbf{v}_e \cdot \nabla(\varphi_e - d_e^2\omega_e) + \mathbf{B}\cdot\nabla j = (-1)^{\nu-1}\eta_\nu \nabla^{2(\nu-1)}\omega_e\,,$$
$$j = \nabla^2\psi, \qquad \omega_e = \nabla^2\varphi_e\,. \tag{2}$$

Since $\nabla \cdot \mathbf{v}_e = \nabla \cdot \mathbf{j} = 0$, the density is time independent for $\nabla n = 0$ initially. The electron pressure is finite but drops out of the equations without further assumption as does any spatially homogeneous axial field B_z. Here we have used the normalizations $x \to x/L$, $t \to t/t_w$, where $t_w = L^2/d_e^2\Omega_e$ is the whistler time, $\varphi_e \to \varphi_e/B_0, \psi \to \psi/LB_0$, where B_0 is a typical poloidal field, and $d_e \to d_e/L$. We have also introduced generalized dissipation terms η_ν, $\nu = 1$ corresponding to resistivity and $\nu = 2$ to (perpendicular) electron viscosity.

We consider stationary reconnection in the framework of Eqs. (1) and (2) with x and y defining the inflow and outflow directions, respectively. For $|x| \gg d_e$ the stationary equations with the reconnection electric field $E = \partial_t\psi =$ const, are (neglecting dissipation)

$$E + \mathbf{v}_e \cdot \nabla\psi = 0\,, \tag{3}$$

$$\mathbf{B}\cdot\nabla j = 0\,, \tag{4}$$

which have the similarity solution [10]

$$\psi = \tfrac{1}{2}(x^2 - a^2y^2)\,, \tag{5}$$

$$\varphi_e = \frac{E}{2a}\ln\left|\frac{x + ay}{x - ay}\right|\,. \tag{6}$$

The upstream flow converges toward the X point, and the downstream flow diverges away from it. Finite η_ν is only needed to smooth the flow singularity on the separatrix $x = \pm ay$. The scale parameter a allows a finite uniform current density, so that the separatrix branches may intersect at any finite angle.

We now show that the solutions (5) and (6) in the region $|x| > d_e$ remain valid when matched to the inertia dominated region $|x| < d_e$, where ψ and φ_e deviate from the expressions (5) and (6). This is in contrast to the resistive MHD behavior where the diffusion region

 0031-9007/95/75(21)/3850(4)$06.00

consists of a macroscopic current sheet, which completely alters the external solution. In the limit of weak collisions the current layer develops a complex multiscale structure. At the smallest scale the current density develops a cusplike singularity as a result of the stagnation of the flow at the X point [3]. The singularity is logarithmic [4], so that its integrated current contribution is zero and its presence does not impact the reconnection rate. At larger scales the current density is driven by E in a region of width δ (along x) and length Δ (along y). We show analytically and numerically that the integrated current in this layer also goes to zero as $d_e \rightarrow 0$. Thus, the magnetic field around the neutral point retains the analytic form given in (5) for any E. The external macroscopic dynamics therefore control E, allowing $E \sim 1$. The calculation of the scaling of the current layer during steady reconnection is straightforward. From the convective terms in the ψ equation we have $B_y \sim j\delta \sim d_e^2 j/\delta$, so $\delta \sim d_e$. The surface integral of the vorticity equation over one quadrant of the current layer yields the outflow velocity $v_0 \sim B_y/d_e \sim j$, the EMHD equivalent of the MHD Alfvén outflow condition. The equality of v_0 and j results from the rotation of j into the outflow direction by B_x. The continuity of the flow into and out of the layer yields $v_0 d_e \sim v_i \Delta$ with v_i the inflow velocity. This can be combined with the inflow velocity $v_i \sim E/B_y$ from (1) to yield $j d_e \sim (E\Delta)^{1/2}$. Finally, canonical momentum conservation along the outflow from (1) yields another relation between j and Δ, $\psi(\Delta) \sim B_x'\Delta^2 \sim \Delta^2 \sim d_e^2 j$, where $B_x' \sim 1$. The final scaling laws for the current layer are then given by

$$\delta \sim d_e, \qquad \Delta \sim (E d_e^2)^{1/3}, \tag{7}$$
$$j \sim v_0 \sim (E/d_e)^{2/3}, \qquad v_i \sim (E/d_e)^{1/3}.$$

Again, since $B_y \sim j\delta \rightarrow 0$ as $d_e \rightarrow 0$, the electron dynamics do not limit the rate of reconnection. A second important result is that the length of the layer is microscopic rather than macroscopic as in resistive MHD.

These results are supported by numerical simulations using Eqs. (1) and (2). We consider the coalescence of two flux bundles located on the diagonal in a square box of edge size $L = 2\pi$:

$$\psi = \exp\{-[(x - x_1)^2 + (y - y_1)^2]^2/4\} + \exp\{-[(x - x_2)^2 + (y - y_2)^2]^2/4\}, \tag{8}$$

where $x_1 = y_1 = \pi/2 + 0.2$, $x_2 = y_2 = 3\pi/2 - 0.2$. The calculations are performed using a psedospectral method. The number of modes N^2 is chosen to provide adequate spatial resolution, varying from 256^2 to 2048^2. We typically take $\nu = 3$ in order to concentrate dissipation at the highest wave numbers. Figures 1(a) and 1(b) show enlargements of $\psi(x,y)$ and $\varphi_e(x,y)$ around the X point during the coalescence of the flux bundles. The X-point structure of ψ and the converging pattern of φ_e are consistent with the solutions (5) and (6). As a result of the acceleration of the flow toward the X point, there is no pileup of flux upstream of the X point as occurs in the MHD case at low resistivity. Similar behavior has been seen in Ref. [3]. The inertia dominated region appears as a small layer of high velocity around the X point. Decreasing d_e reduces the size of this region along both the inflow and outflow directions [Fig. 1(c)] consistent with the scaling laws (7). The flux reconnection rate E is found to be independent of d_e and η_3, which have been varied over the intervals $10^{-1} \leq d_e \leq 10^{-2}$ and $10^{-6} \leq \eta_3 \leq 10^{-11}$.

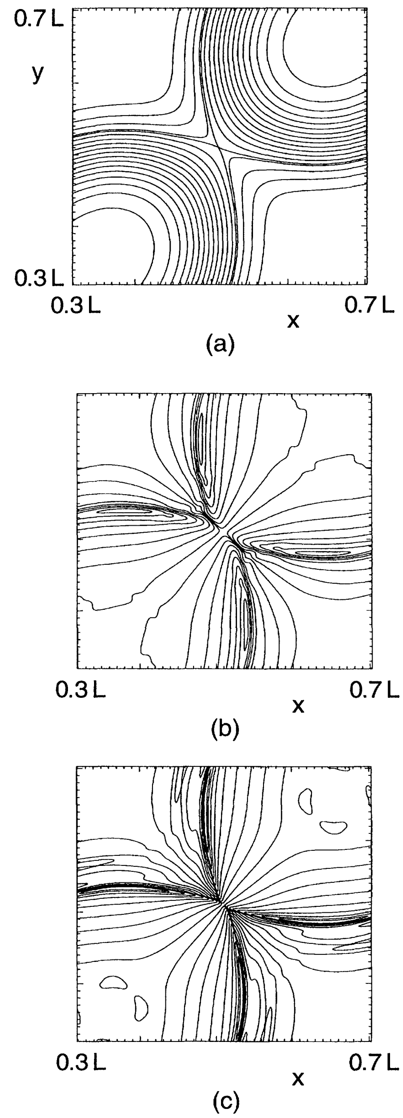

FIG. 1. Coalescence of two magnetic flux bundles in EMHD. Blowups around the X point showing (a) ψ and (b) φ_e for $d_e = 0.06$; and (c) φ_e for $d_e = 0.015$, ψ being partically identical to (a).

At scale lengths larger than d_i ions and electrons move essentially together. To include the ions in a simple model, we assume that their motion is incompressible and introduce the ion stream function φ_i, $\mathbf{v}_i = \hat{\mathbf{z}} \times \nabla\varphi_i$, $\omega_i = \nabla^2\varphi_i$. The incompressibility assumption is valid, when the characteristic reconnection velocities are slow compared with the magnetosonic speed. For simplicity, we consider only the high-β case, where the ion pressure equation yields $\nabla \cdot \mathbf{v}_i = 0$ and compressibility terms of the form $B_z\nabla \cdot \mathbf{v}_e$ in Eq. (2) can hence be neglected.

Adding the equations of motion of ions and electrons gives

$$d_i^2(\partial_t\omega_i + \mathbf{v}_i \cdot \nabla\omega_i) + d_e^2(\partial_t\omega_e + \mathbf{v}_e \cdot \nabla\omega_e) - \mathbf{B} \cdot \nabla j = (-1)^\nu[\mu_\nu\nabla^{2(\nu-1)}\omega_i + \eta_\nu\nabla^{2(\nu-1)}\omega_e]. \tag{9}$$

Neglecting the axial velocity of the ions compared with that of the electrons, the axial current density j remains unchanged and so does Eq. (1) for ψ. The poloidal current density is, however, modified, $\mathbf{j} = -\hat{\mathbf{z}} \times \nabla\delta B_z = \hat{\mathbf{z}} \times \nabla(\varphi_i - \varphi_e)$, so $\delta B_z = \varphi_e - \varphi_i$. Equation (2) then becomes

$$\partial_t(\varphi_e - \varphi_i - d_e^2\omega_e) + \mathbf{v}_e \cdot \nabla(\varphi_e - \varphi_i - d_e^2\omega_e) + \mathbf{B} \cdot \nabla j = (-1)^\nu\eta_\nu\nabla^{2(\nu-1)}\omega_e. \tag{10}$$

Equations (1), (9), and (10) have been solved numerically for the same initial state (7). Since it is difficult to combine the most interesting case $d_i \ll 1$ with a realistic ratio $d_i/d_e = \sqrt{m_i/m_e} \sim 50$, we choose values $d_i/d_e \sim 10$, varying both d_i and d_i/d_e, $0.4 \geq d_i \geq 0.025$, $13.3 \geq d_i/d_e \geq 6.6$, to obtain the relevant scaling behavior. Figure 2 shows a typical state from a simulation run with $d_i = 0.1$, $d_e = 0.015$, $\eta_3 = \mu_3 = 4 \times 10^{-10}$. It can be seen by comparing φ_e and φ_i contours that at large distances from the X point (and the separatrix) ion and electron flow patterns are very similar. They differ, however, in the vicinity of the X point, where ion spatial scales ($\sim d_i$) are much larger than those of the electrons ($\sim d_e$). For $|x| < d_i$ the electron flow again shows the converging pattern as in the EMHD case.

Table I gives the maximum reconnection rate $E_{\max}$ and the time t_0 required for complete coalescence for several different runs. The reconnection rate depends only on d_i, i.e., the ion mass, being independent of both d_e and the dissipation coefficients. For not too small values of d_i, $1 > d_i \gtrsim 0.1$, we find the scaling $E_{\max} \sim d_i^{-1}$. Since the time unit in these simulations is the whistler time t_w, which is related to the Alfvén time $t_A = L\sqrt{4\pi n m_i}/B_0$ by $t_A/t_w = d_i$, reconnection in this range is Alfvénic depending only on the global configuration. For smaller values of d_i the reconnection rate is slower than Alfvénic. Though the asymptotic behavior for $d_i \rightarrow 0$ cannot be unambiguously inferred from the data in Table I, it appears that the reconnection rate approaches a constant corresponding to an inflow velocity $v_i \sim d_i v_A/L$, which implies that the ions form a macroscopic Sweet-Parker-like layer with a width d_i and outflow velocity v_A.

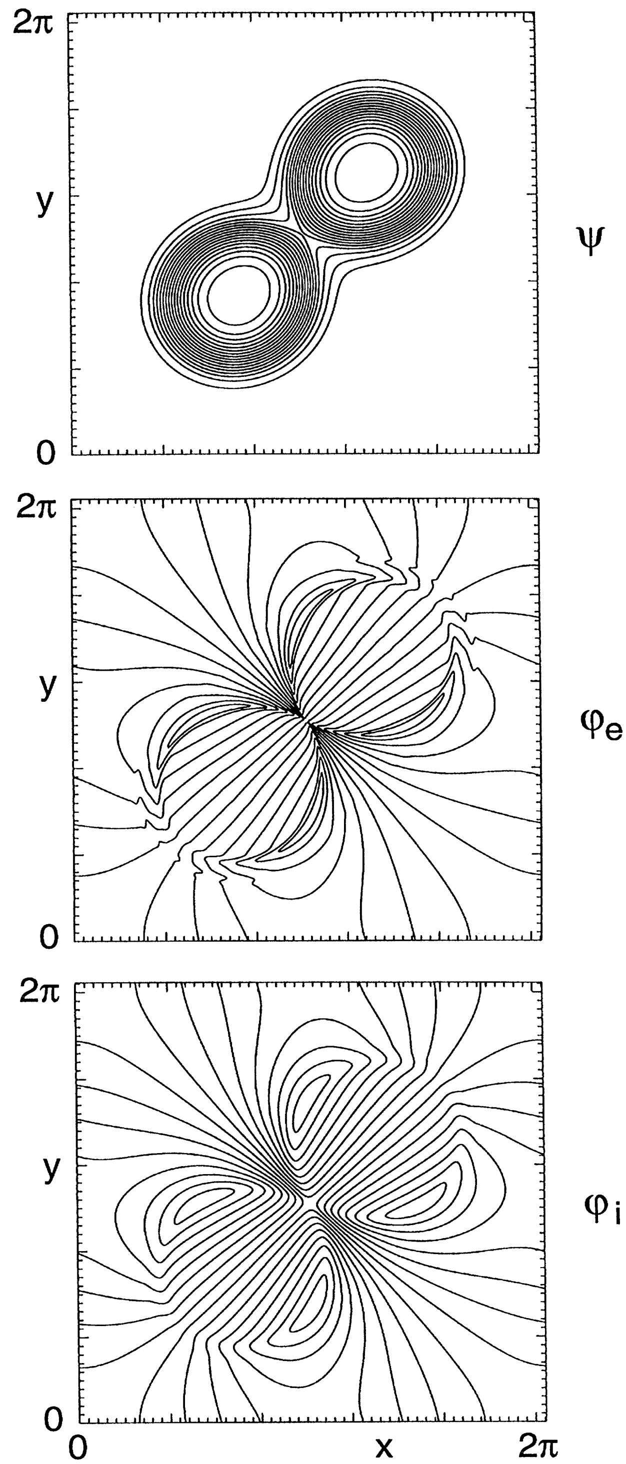

FIG. 2. Coalescence of two flux bundles including the ion dynamics, $d_i = 0.1$ and $d_e = 0.015$.

Finally, to demonstrate that the decoupling of the electron and ion motion by the Hall term fundamentally alters the reconnection process, we switch off the Hall term

TABLE I. Summary of results of different simulation runs including the ion dynamics.

d_i	d_e	η_3	$E_{\max}$	t_0
∞	0.03	10^{-8}	1.4	1.5
0.4	0.03	4×10^{-10}	1.7	1.3
0.2	0.03	10^{-8}	2.5	1.0
0.2	0.015	10^{-8}	2.4	1.0
0.2	0.03	4×10^{-10}	2.4	1.0
0.1	0.015	10^{-8}	4.4	0.5
0.1	0.015	4×10^{-10}	4.4	0.55
0.05	0.0075	4×10^{-10}	6.7	0.35
0.025	0.0075	1×10^{-10}	8.6	0.26

setting $\varphi_e = \varphi_i = \varphi$ but keep finite electron inertia in Eq. (1). This model has previously been used in studies of collisionless reconnection [2,3]. In this case the flow pattern is changed significantly, since the ions are now forced into a narrow sheet of width d_e. The reconnection rate is much slower than in the corresponding case including the Hall term. Varying d_e we find that the reconnection rate depends strongly on d_e, roughly $E_{\max} \sim d_e$.

In conclusion, we have shown that the Hall term in Ohm's law has a dramatic effect on the dynamics of magnetic reconnection in collisionless plasmas. The electron and ion motion decouple on scale lengths of order c/ω_{pi} around the dissipation region, allowing the reconnection rate to become independent of the electron mass and thus to depend only on the ion dynamics. The resulting merging rates greatly exceed those based on reconnection controlled by electrons. The results also resolve the long-standing controversy over whether the electrons or ions control magnetic reconnection in the Earth's magnetotail.

The calculations presented are based on the fluid description, which does not properly describe wave-particle resonances or finite Larmor radius effects. In the linear regime the collisionless tearing mode is strongly affected by electron thermal streaming, and the fluid treatment is not correct. Once an X-point configuration forms, particle simulations [11] show that the magnetic field constrains the electron thermal streaming motion and the system evolves to a fluid-dominated regime, in which neither the thermal Larmor radius nor parallel streaming is important. The fluid model does not, of course, allow us to correctly describe the energy partition between fast and slow particles, which is important in understanding energetic particle signatures during magnetic reconnection in both the Earth's magnetosphere and in the solar corona. The study of the test particle dynamics in the fields produced by fluid reconnection simulations could shed light on this problem. Full particle simulations of sufficient resolution to properly separate the relevant scale lengths must await future massively parallel computers.

[1] See, e.g., A.M. Edwards *et al.*, Phys. Rev. Lett. **57**, 210 (1986).
[2] V.M. Vasyliunas, Rev. Geophys. **13**, 303 (1975).
[3] J.F. Drake and R.G. Kleva, Phys. Rev. Lett. **66**, 1458 (1991).
[4] M. Ottaviani and F. Porcelli, Phys. Rev. Lett. **71**, 3802 (1993).
[5] See, e.g., D. Biskamp, Phys. Rep. **237**, 181 (1994).
[6] M.E. Mandt, R.E. Denton, and J.F. Drake, Geophys. Res. Lett. **21**, 73 (1994).
[7] A.S. Kingsep, K.V. Chukbar, and V.V. Yan'kov, in *Reviews of Plasma Physics* (Consultants Bureau, New York, 1990), Vol. 16.
[8] S.V. Bulanov, F. Pegoraro, and A.S. Sakharov, Phys. Fluids B **4**, 2499 (1992).
[9] J.F. Drake, R.G. Kleva, and M.E. Mandt, Phys. Rev. Lett. **73**, 1251 (1994).
[10] D. Biskamp, Phys. Fluids **29**, 1520 (1986).
[11] J.R. Burkhardt, J.F. Drake, and J. Chen, J. Geophys. Res. **96**, 11 539 (1991).